Phonon-focusing effect with laser-generated ultrasonic surface waves

Al. A. Kolomenskii and A. A. Maznev
General Physics Institute, Vavilov Street 38, 117942 Moscow, Russia
(Received 21 June 1993)

Surface-phonon focusing is examined with laser generation of pulsed surface acoustic waves (SAW's). Before presentation of the experimental results, the theory of the effect is summarized including both the ray approach and the stationary-phase analysis. To create a point source of SAW's the focused beam of a Q-switched Nd:YAG (yttrium aluminum garnet) laser is employed. To visualize the SAW amplitude distribution we use dust patterns arising as a result of SAW-induced dust-particle removal from the surface under investigation. The SAW amplitude measurements with the probe beam deflection technique show that the above patterns reflect adequately the SAW amplitude angular dependence. The strong SAW focusing is observed on cubic crystals such as Si, Ge, GaAs, as well as on $LiNbO_3$ crystal. The results obtained are discussed in comparison with the theory.

I. INTRODUCTION

The distinct anisotropy of acoustic energy flux from a point source acting in an anisotropic elastic solid is referred to as phonon focusing. There has been considerable work on this effect in the area of ballistic transport of bulk thermal phonons. Observed by Taylor, Maris, and Elbaum,[1] focusing of ballistic phonons was then investigated by many authors,[2] and close agreement between experiment and theory was achieved.

Relatively little attention has been given to the effect in question with ultrasonic waves. It seems to be connected with the fact that traditional acoustics does not generally deal with point sources of ultrasound. Meanwhile, such a source is easily realized using laser generation of acoustic waves.[3] Recently, focusing of laser-generated ultrasonic bulk waves has been reported by Every *et al.*,[4] while Hauser, Weaver, and Wolfe[5] used a version of scanning acoustic microscopy technique for that purpose.

Surface acoustic waves (SAW's) can also be focused, as has been shown theoretically by several authors.[6–10] In particular, calculations for some cubic crystals were presented in Ref. 7. As far as we know, however, phonon focusing of SAW's has never been observed directly. It should be noted that an idea to use laser excitation of SAW's to observe SAW focusing was proposed by Novikov and Chernozatonskii.[10]

In the present paper[11] we report experimental results for the phonon-focusing effect, with SAW pulses generated by laser irradiation. Principal attention is paid to cubic crystals such as Si, Ge, and GaAs, and a strong focusing of SAW's is found to occur in these crystals. This effect is also observed in the y cut of $LiNbO_3$ crystal. We present as well a comparison of experimental results obtained with theoretical speculations.

II. THEORY

We consider first an approach of geometrical acoustics. The origin of the SAW focusing effect is the SAW phase velocity anisotropy resulting in a deviation of the group velocity of SAW from its phase velocity. The modulus v and direction φ of the SAW group velocity are expressed through c and θ of the phase velocity as follows:[12]

$$v=[c^2+(dc/d\theta)^2]^{1/2}, \tag{1}$$

$$\varphi=\theta+\tan^{-1}\left[\frac{1}{c}\frac{dc}{d\theta}\right]. \tag{2}$$

As the acoustic energy propagates along the group velocity directions, the measure of the ray density anisotropy is provided by the focusing factor[1,9]

$$A=\left|\frac{d\varphi}{d\theta}\right|^{-1}. \tag{3}$$

Qualitatively, strong focusing occurs when the group velocity direction remains the same, while the phase velocity direction varies. Using Eq. (2) factor A can be expressed by

$$A=\frac{1+c'^2/c^2}{|1+c''/c|}, \tag{4}$$

where $c'=dc/d\theta$, and $c''=d^2c/d\theta^2$. The SAW amplitude far from the source must be proportional to $A^{1/2}$. Since $c'^2/c^2\ll 1$ holds as a rule, the main angular dependence of the SAW amplitude u is given by

$$u\approx|1+c''c/c|^{-1/2}. \tag{5}$$

In crystal cuts with sufficiently strong anisotropy it is possible for singular directions defined by the condition

$$c''/c=-1 \tag{6}$$

to exist, in which case the focusing factor A becomes infinite. The above condition readily can be shown to define points at which the curvature of the SAW slowness curve vanishes. It should be noted that Eq. (6) coincides with the condition of diffraction-free propagation of a finite-aperture beam of SAW's.[13]

The existence of singularities is certainly due to the restricted nature of the ray approach used above. A more

strict approach based on the wave propagation theory is developed in Refs. 6 and 7 dealing with the Green's function of an anisotropic elastic half-space, derived from equations of elasticity with boundary conditions at a free surface. However, we believe that consideration from a more general point of view would be of interest, regarding not only SAW's but also two-dimensional waves of any type with phase velocity anisotropy. Let us consider two-dimensional wave field $u(\mathbf{r},t)$, where $\mathbf{r}=(x,y)$, generated by a source of arbitrary appearance localized near $\mathbf{r}=0$. Disregarding dissipation and dispersion, in the far field of the source $u(\mathbf{r},t)$ can be represented as a superposition of plane sinusoidal waves:

$$u(\mathbf{r},t)=\int B(\mathbf{k})\exp[i\mathbf{k}\mathbf{r}-kc(\vartheta)t]d\mathbf{k} , \tag{7}$$

where k and ϑ are the modulus and angle, respectively, of the wave vector $\mathbf{k}$, $c(\vartheta)$ is the angular dependence of the phase velocity, and $B(\mathbf{k})$ is the partial-wave amplitude determined by the concrete appearance of the source. Using polar coordinates r and φ, and making a substitution $k\rightarrow\omega/c(\vartheta)$, we obtain

$$u(r,\varphi,t)=c^{-2}\int_0^{\infty}d\omega\int_0^{2\pi}d\vartheta\,\omega F(\omega,\vartheta)\exp\left[i\omega\left[\frac{r\cos(\vartheta-\varphi)}{c(\vartheta)}-t\right]\right] , \tag{8}$$

where $F(\omega,\vartheta)=B[\omega\cos(\vartheta)/c(\vartheta),\omega\sin(\vartheta)/c(\vartheta)]$.

In order to obtain the asymptotic of the integrand for large r we use, similarly to Refs. 6 and 7, the method of stationary phase. The result is

$$u=c^{-2}\int_0^{\infty}d\omega\,\omega F(\omega,\theta)\exp\{i\omega[r/v(\theta)-t]\}\times\int_{-\infty}^{\infty}d\xi\exp\left[i\omega r\left[\tfrac{1}{2}a_2\xi^2+\frac{1}{(3!)}a_3\xi^3+\cdots\right]\right] , \tag{9}$$

where the stationary point $\vartheta=\theta$ is defined by Eq. (2), v is the modulus of the group velocity defined by Eq. (1), and a_n is the n-order derivative of $[\cos(\vartheta-\varphi)/c(\vartheta)]$ with respect to ϑ at $\vartheta=\theta$. In particular, $a_2=-c^{-1}(c^2+c'^2)^{-1/2}(c+c'')$.

If $c''/c\neq-1$, we keep only the first term in the exponent and, integrating over ξ, obtain

$$u=c^{-2}\left[\frac{2\pi[1+c'^2/c^2]^{1/2}}{rc|1+c''/c|}\right]^{1/2}\times\int_0^{\infty}d\omega\,\omega^{1/2}F(\omega,\theta)\times\exp[i\omega(r/v-t)-\mathrm{sgn}(c''+c)i\pi/4] . \tag{10}$$

If $F(\omega,\theta)$ depends weakly on θ, as may be expected for a source with axial symmetry, the main angular dependence of the wave amplitude is given again by Eq. (5).

Of especial interest are singular directions, defined by Eq. (6), at which a_2 vanishes. It has been stated[6,7] that if $a_2=0$ and $a_3\neq0$ then the dependence of the amplitude on the distance is proportional to $r^{-1/3}$, as opposed to dependence $r^{-1/2}$ in the nonsingular case described by Eq. (10). In Refs. 9 and 10 the realizability of the case $a_2=a_2=0$ and $a_4\neq0$ has been shown, when $u\sim r^{-1/4}$ holds. Let us consider the general instance when the first nonzero term is a a_N. This can be shown to be the case under conditions

$$c^{(n)}+c^{(n-2)}\begin{cases}=0, & n<N\\ \neq0, & n=N\end{cases} , \tag{11}$$

where $c^{(n)}=d^nc/d\theta^n$, and a_N can then be found to be equal to $-c^{-1}(c^2+c'^2)^{-1/2}(c^{(N-2)}+c^{(N)})$. The integral over ξ in Eq. (9) can be carried out in this case with the result that

$$u=2c^{-2}\Gamma(1+1/N)\left[\frac{N!(c^2+c'^2)^{1/2}}{c|c^{(N-2)}+c^{(N)}|}\right]^{1/N}r^{-1/N}\int_0^{\infty}d\omega\,\omega^{1-1/N}F(k,\theta)\exp[i\omega(r/v-t)]\times\begin{cases}\exp(-\mathrm{sgn}(c^{(N-2)}+c^{(N)})i\pi/2N) & \text{if } N \text{ is even}\\ \cos(\pi/2N) & \text{if } N \text{ is odd} ,\end{cases} \tag{12}$$

where Γ is the Euler gamma function, so the amplitude is proportional to $r^{-1/N}$.

Finally, it should be noted that in order to analyze the vicinity of a singular direction at a finite distance r we must keep several terms in the exponent of the integrand in Eq. (9). In Ref. 7 the case has been considered when neither a_2 nor a_3 can be neglected, and the integral over ξ has been calculated as being given by an Airy function. This result is a manifestation of a general rule that the amplitude of a monochromatic wave oscillates in the vicinity of a caustic. If, however, a pulsed source with a wide spectrum is used, as was the case in our experiment to be described below, the oscillations are believed to be smoothed over when integrating over ω.

III. EXPERIMENTAL PROCEDURE

To generate SAW pulses, a Q-switched Nd:YAG (yttrium aluminum garnet) laser (wavelength 1.06 μm, pulse duration 10 ns, pulse energy 10 mJ) was used. The laser beam was focused on the surface of a sample using a $f=6$ cm convex lens, with the $1/e$ radius of the focusing spot being equal to 7 μm. Application of the laser pulse to the surface caused an optical breakdown and generated a powerful SAW pulse with a characteristic duration corresponding to that of the laser pulse, as it was measured with the laser probe (see below). The characteristic SAW frequency thus was about 50 MHz.

The qualitative examination of the SAW amplitude anisotropy was accomplished by using the following method of visualization. The sample surface was dusted with 1–2-μm Al_2O_3 particles. Mechanical detachment of the particles from the surface accompanying the passage of an intense SAW was employed.[14] The action of the SAW causes the surface to move with acceleration, and an inertial force acts on a particle at rest in the coordinate system of the surface. If the acceleration of the surface is directed into the sample, and if $w_\perp > F_{ad}/m$, where $w_\perp$ is the normal component of the acceleration, m is the mass of a particle, and F_{ad} is the adhesion force between the particle and the surface, then the particle will detach itself from the surface (in order that the detached particles did not settle back on the surface, in our experiment the surface under examination was positioned vertically). Thus the degree of removal of particles from the surface depends on the SAW amplitude. It should be noted that the surface accelerations in the SAW reached high values $w_\perp \approx 10^8$ m/s^2, so the removal of micron-size particles was possible.[14] In a photograph made with side illumination, the dusty surface appears light, and that cleaned of particles looks dark; such a photograph displays qualitatively the SAW amplitude distribution. Note that it is not a time-resolved technique, as is a photograph taken well after the experiment.

The pictures presented below in this paper were taken after about ten consequent laser shots. Pictures arising after a single laser shot were similar but of poor contrast. Though the sample surface was positioned vertically, a substantial portion of detached particles settled back on the surface,[14] so it took several shots to obtain satisfactory contrast.

To assure that dust patterns correctly reflect SAW amplitude anisotropy, we also carried out direct measurements of the SAW amplitude using a probe beam deflection technique.[15] A beam from a continuous-wave He-Ne laser (wavelength 0.63 μm, power 12 mW) was directed obliquely on the surface and focused into a spot with a radius of 15 μm. After reflection it was recorded using a fast two-sector photodiode, whose signal was proportional to the beam deflection angle. Thus the laser probe recorded the angle of the inclination of the surface, proportional to the normal component of the surface velocity.

An oscilloscope trace of a signal was photographed, and its peak-to-peak amplitude was then measured. Since every laser shot resulted in local surface damage, the Nd:YAG laser spot was moved to a new point on the surface after each shot. The temporal resolution of the technique was 10 ns. From the time delay between the laser pulse and the signal the SAW velocity was calculated in order to check that what we were measuring was a SAW, and not a shock wave in air, reflected bulk wave, etc.

IV. RESULTS AND DISCUSSION

Shown in Fig. 1(a) is a photograph of the dusted (111) surface of a silicon wafer after laser action. Clear-cut dark tracks correspond to those directions in which strong focusing occurs. The pattern reflects the symmetry of the acoustic properties of the (111) surface: the normal to the surface is a threefold axis, and there is a symmetry relative to the center and the ⟨110⟩ axis. For the sake of simplicity we will hereafter describe the variety of symmetrical directions as a single direction. From this point of view we have a single focusing direction making an angle $\varphi=30°$ with the ⟨110⟩ axis.

In Fig. 1(b) the angular dependence of the SAW amplitude measured by using the laser probe is presented. Indeed, a sharp maximum can be seen at $\varphi=30°$. Thus we may conclude that our "dust pattern" reflects correctly the SAW amplitude anisotropy.

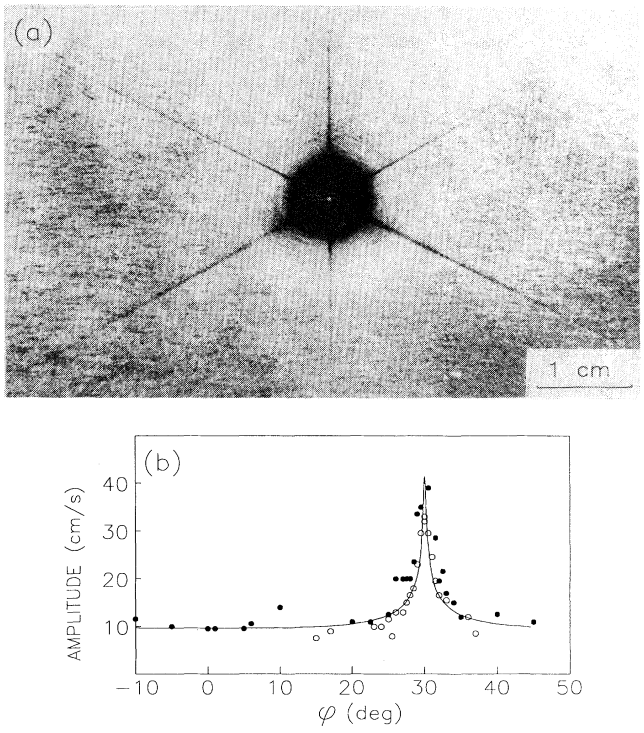

FIG. 1. Phonon focusing of SAW's in the (111) plane of silicon. (a) Focusing pattern: photograph of the dusted surface after laser-acoustic action. The ⟨110⟩ axis is horizontal. (b) Measured and calculated angular dependencies of the amplitude of the normal component of the surface velocity in a SAW pulse. The angle φ is measured from the ⟨110⟩ direction. The black and white circles refer to different series of measurements. For the calculated curve an arbitrary amplitude scale is used.

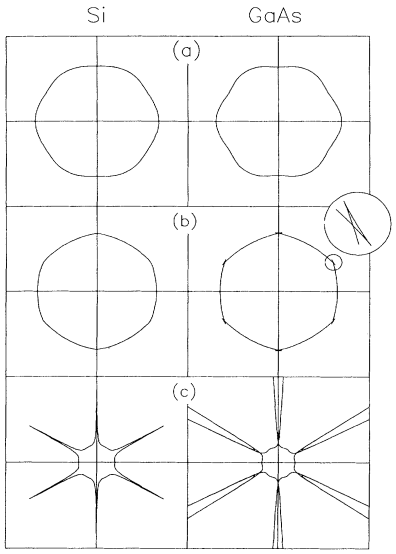

FIG. 2. SAW focusing calculations for the (111) surfaces of Si and GaAs. (a) The SAW slowness curves, (b) the wave fronts of the SAW's propagating from a point source, and (c) the polar plots of the SAW amplitude derived using Eq. (5). The ⟨110⟩ axis is horizontal.

To compare the results obtained with the theory, we have carried out calculations based on the $c(\theta)$ dependence for the (111) silicon surface presented in Ref. 12. The left part of Fig. 2 shows the SAW slowness curve, the SAW wave front, and the polar plot of the SAW amplitude versus the direction of observation for the (111) silicon surface. In the instance under consideration there are no singular directions, since c''/c never reaches the value -1; however, in the direction of maximum SAW velocity $\theta=\varphi=30°$ it is very close to this value ($c''/c|_{\theta=30°}=-0.92$), thereby rather strong focusing occurs in this direction. The theoretical angular dependence of the SAW amplitude is also represented in Fig. 1(b), showing good agreement with the experimental data.

It is also of interest to examine the (111) surface of a cubic crystal with stronger anisotropy, where caustics must appear. We have chosen GaAs as an example, whose anisotropy factor $\eta=2c_{44}/(c_{11}-c_{12})=1.8$ is considerably larger compared to that of silicon ($\eta=1.56$).[12] In the right part of Fig. 2 the results for the (111) surface of GaAs are presented, being calculated again on the basis of the $c(\theta)$ dependence from Ref. 12. Concave sections of the slowness curve can be seen, which cause cusps of the SAW wave front. The singular directions

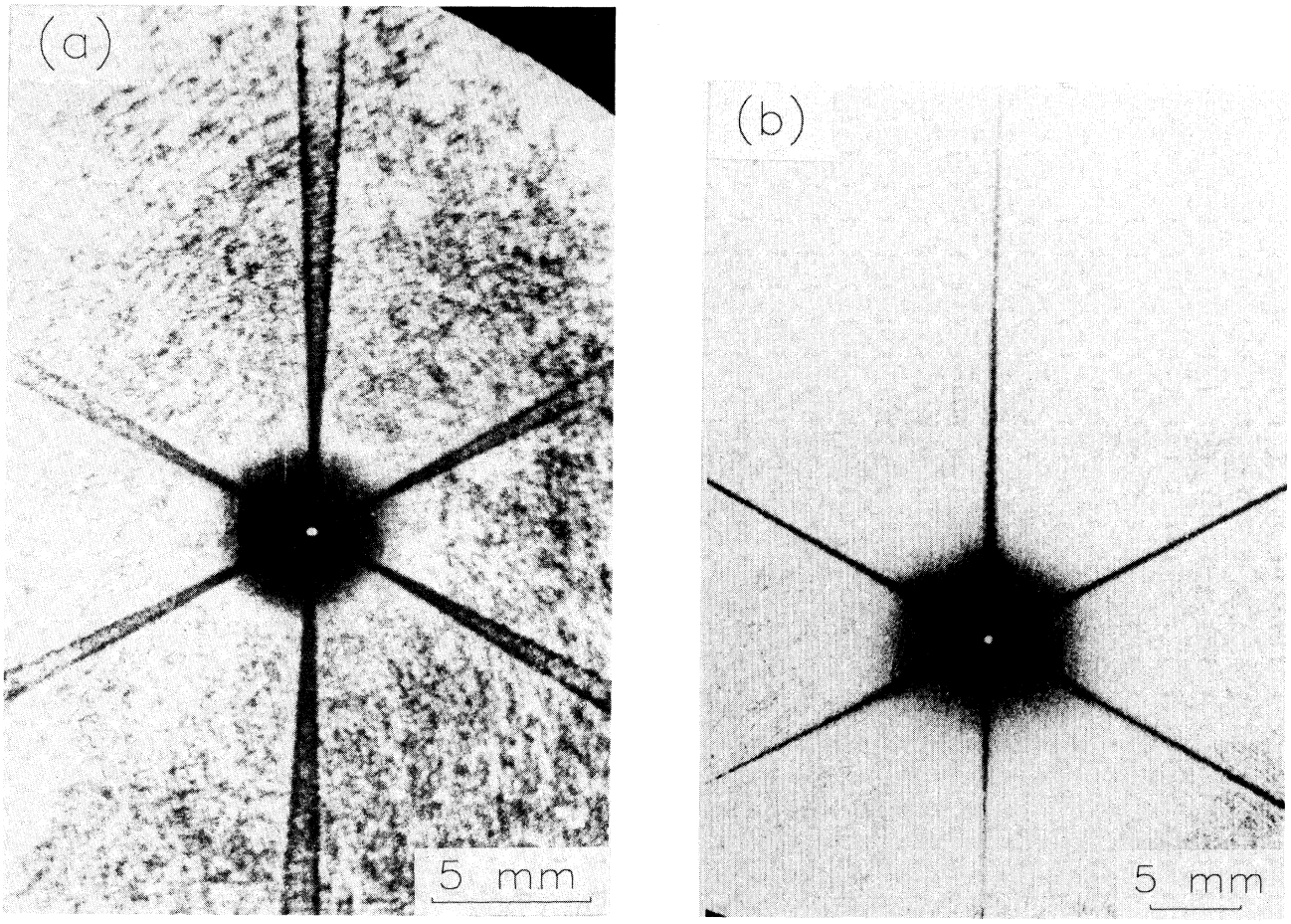

FIG. 3. Focusing patterns for the (111) surfaces of (a) GaAs and (b) germanium. The ⟨110⟩ axis is horizontal.

(caustics), at which the focusing factor A becomes infinite, correspond to the cusps and are positioned symmetrically near the direction $\varphi=30°$. Previously the singular focusing directions in the (111) cut of GaAs were calculated by Chernozatonskii and Novikov,[10] and our results are in agreement with theirs.

The focusing pattern for the (111) GaAs surface obtained by us experimentally is shown in Fig. 3(a). Agreement between theory and experiment can be seen to be good.

We have also obtained the focusing pattern for the (111) surface of Ge [see Fig. 3(b)]. It seems to be similar to that for the (111) silicon surface. Actually, the ratios of elastic constants are close for these two crystals [e.g., $\eta=1.66$ for Ge (Ref. 12)]. Nevertheless, results by Camley and Maradudin[7] show that the singular focusing has to occur in the (111) cut of Ge, with the angle between caustics $\approx 1°$. Data from Ref. 10 as well as calculations carried out by us confirm this result. The pattern obtained experimentally, however, shows the nonsplitting focusing directions, so the angle between caustics cannot exceed 0.3°. At present we cannot explain this discrepancy between theory and experiment.

We also examined the SAW focusing in the (100) and (110) cuts of silicon. Corresponding focusing patterns are presented in Fig. 4. Let us first consider the (100) surface. Here we can see a distinct maximum making the angle $\varphi=20°$ with the $\langle 110\rangle$ axis. Also, a weaker side track can be seen. This is in agreement with the angular dependence of the SAW amplitude measured with the laser probe.[11] However, a strange feature is that the side track seems not to pass through the center.

The results of calculations based on the $c(\theta)$ data for the (100) cut of silicon from Ref. 16 are presented in Fig. 5. The angular dependence of the SAW amplitude obtained is similar to that for the (100) surface of Ge calculated by Camley and Maradudin.[7] In this instance a singular focusing occurs, and directions of caustics with respect to the $\langle 110\rangle$ axis were calculated as $\varphi_1=20°$ and $\varphi_2=30°$. While the former was actually observed, the latter was not displayed in the experiment.

This contradiction is believed to be due to the fact that the angular dependence of the SAW amplitude is determined not only by the focusing effect, but also by the angular dependence of the spectral component $F(\omega,\theta)$. The calculation of $F(\omega,\theta)$ for the ablation regime of laser generation of SAW's is rather complicated and is beyond the scope of our consideration. Nevertheless, some quali-

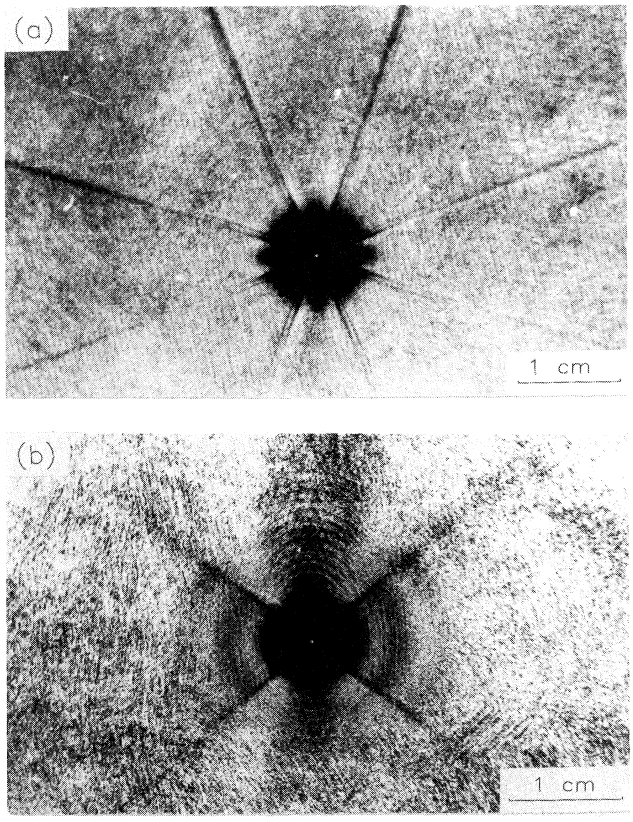

FIG. 4. Focusing patterns for the (a) (100) and (b) (110) surfaces of Si. In the both cases the $\langle 110\rangle$ axis is horizontal.

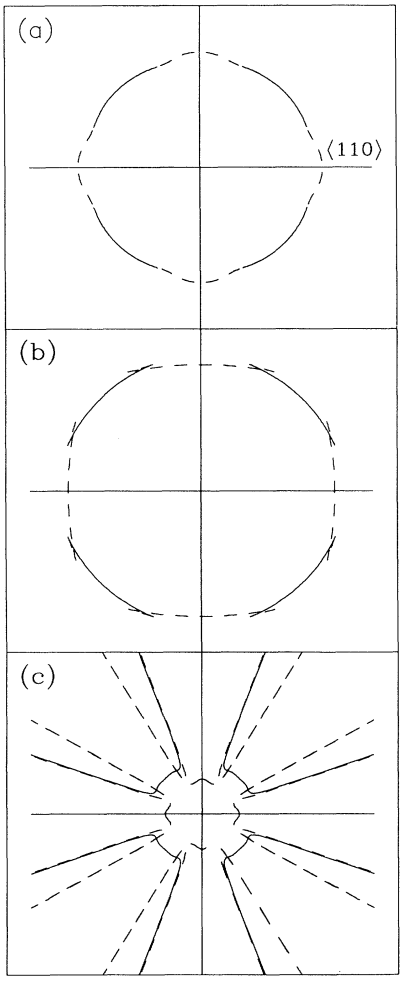

FIG. 5. (a) The slowness curve, (b) the SAW wave front, and (c) the polar plot of the SAW amplitude for the (100) surface of Si.

tative analysis can be made. It is known[16,17] that in the vicinity of the ⟨110⟩ direction the Rayleigh wave couples with the slowest bulk shear wave. This coupling, occurring at the phase velocity angle $\theta \approx 15°$,[16,18] leads to strong attenuation of the laser-generated SAW amplitude.[18] Let us assume that in our case the SAW amplitude vanishes for $\theta < 15°$. Corresponding sections of the curves in Fig. 5 are plotted as dashed lines. It can be seen from Fig. 5(c) that the absence of a maximum at $\varphi = 30°$ in the experimental pattern can be recognized in such a way. The origin of the weak side track, however, is not yet clear. Also, it should be noted that while the Rayleigh wave transforms into the bulk shear one, another Rayleigh-type wave (referred to as a pseudosurface or leaky wave) arises in the vicinity of the ⟨110⟩ direction.[16,17] The directivity pattern lobe corresponding to this wave also can be seen to be displayed in the focusing pattern observed [Fig. 4(a)].

The focusing pattern for the (110) surface of silicon is presented in Fig. 4(b). It is in agreement with the calculations for the (110) surface of Ge.[7] At this point we have nonsingular focusing, and there is a weak maximum at $\varphi = 42°$ with respect to the ⟨110⟩ direction. One could notice ring structures which are visible in Fig. 4(b). The small-scale structures seem to be parallel to the SAW wave fronts, and were also observed by us in the (111) as well as (100) planes of Si, though not so distinctly. The origin of these structures is not clear as yet. Being beyond the scope of the present paper, this question seems to be of some interest.

One can also see large dark and light rings in Fig. 4(b). We suppose that these result from the finite thickness (0.5 mm) of the silicon wafer. The Rayleigh wave in a plate can be represented as a sum of the lowest symmetric and antisymmetric Lamb's plate modes.[19] The dispersion of these modes can cause the wave to transit periodically from one side of the plate to another,[19] leading to SAW amplitude oscillations.

The question is whether it is correct to compare the results obtained with thin wafers with the calculations for SAW's in a semi-infinite solid. Indeed, all our silicon samples were of 0.5-mm thickness, while other samples were more than 2 mm thick. It should be noted, however, that even for silicon wafers $kh \approx 30 \gg 1$ for a 50-MHz SAW, where k is the acoustic wave vector and h is the wafer thickness. Thus we believe that the wave observed is close enough to a pure surface so that the dispersion, though observable, does not substantially affect the angular dependence of the phase velocity. This is confirmed by the close agreement between experimental results and calculations for the (111) silicon waver [see Fig. 1(b)]. Still we would consider it useful to check our results with bulk samples.

As for thick samples, the question may be raised as to whether reflected bulk waves can contribute to the "dust patterns" observed. We believe it not to be the case, as no patterns were observed on the opposite sides of the samples. This is due to the fact that bulk wave amplitude decreases with distance as $1/r$, i.e., faster than that of the surface wave.

We have examined the SAW focusing on three basic surfaces of cubic crystals. In addition, let us consider the focusing in the y cut of the $LiNbO_3$ crystal, taking into account the importance of this material which is frequently used as a substrate for SAW's. The focusing pattern obtained in this case is shown in Fig. 6. The only focusing direction can be seen to be parallel to the z axis. It is in agreement with the theory because, in the y cut of $LiNbO_3$, c''/c is known[13] to be close to -1 in the z direction [the exact value is -1.083 (Ref. 13)].

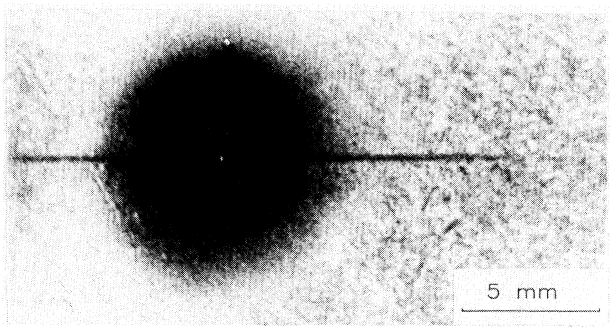

FIG. 6. Focusing pattern for the y cut of the $LiNbO_3$ crystal. The z axis is horizontal.

V. CONCLUSION

The surface-phonon focusing effect was observed using laser generation of SAW pulses.

Experimental results were preceded by a summary of the theory of two-dimensional phonon focusing, including both the ray approach and stationary-phase analysis with somewhat different terms as compared to earlier papers,[6,7] thus making the analysis more simple and straightforward.

The focused beam of a Q-switched Nd:YAG laser was employed to create a point source of 10-ns-duration SAW pulses. To examine the focusing effect we used a method of visualization of the SAW amplitude distribution based on the SAW-induced dust removal. The SAW amplitude measurements with the probe beam deflection technique showed that the dust patterns reflect correctly the angular dependence of the SAW amplitude.

Principal attention was paid to cubic crystals. The (111), (100), and (110) surfaces of silicon as well as the (111) surfaces of Ge and GaAs were examined. A general conclusion may be drawn that on the whole the results obtained agree with the theory, in particular with the results for cubic crystals obtained by Camley and Maradudin.[7] For the (111) surface the transition from nonsingular to singular focusing was observed when the anisotropy factor increased. For the (100) plane some feature resulting from the coupling of the Rayleigh wave with the bulk shear one was found. Some discrepancies between experiment and theory have been pointed out. In addition, SAW focusing in the y cut of $LiNbO_3$ has been observed.

Finally, we should like to note that the experimental technique we used for the SAW focusing examination is

much simpler than that used to examine the bulk wave focusing with either ballistic phonons[2] or ultrasonic waves.[5] We believe the SAW focusing study should be continued, as it is of interest from the points of view both of theory and application.

ACKNOWLEDGMENTS

The authors would like to thank Dr. E. I. Shklovskii for his help during early stages of this work, and Professor F. V. Bunkin for a discussion of the results.

[1]B. Taylor, H. J. Maris, and C. Elbaum, Phys. Rev. Lett. **23**, 416 (1969); Phys. Rev. B **3**, 1462 (1971).

[2]See, for a review, G. A. Nortrop and J. P. Wolfe, in *Nonequilibrium Phonon Dynamics,* edited by W. E. Bron (Plenum, New York, 1985).

[3]For a review see, e.g., F. V. Bunkin, Al. A. Kolomenskii, and V. G. Mikhalevich, in *Lasers in Acoustics,* Vol. 12 of *Laser Science and Technology,* edited by H. Walther and V. S. Letokhov (Harwood, Chur, Switzerland, 1991). Laser generation of SAW's is reviewed in A. A. Karabutov, Usp. Phys Nauk **147**, 605 (1985) [Sov. Phys. Usp. **28**, 1042 (1985)].

[4]A. G. Every, Wolfgang Sachse, K. Y. Kim, and M. O. Thompson, Phys. Rev. Lett. **65**, 1446 (1990); A. G. Every and Wolfgang Sachse, Phys. Rev. B **44**, 6689 (1991).

[5]Matt R. Hauser, R. L. Weaver, and J. P. Wolfe, Phys. Rev. Lett. **68**, 2604 (1992).

[6]H. Shirasaki and T. Makimoto, J. Appl. Phys. **49**, 658 (1978); **49**, 661 (1978); **50**, 2795 (1979).

[7]R. E. Camley and A. A. Maradudin, Phys. Rev. B **27**, 1959 (1983).

[8]S. Tamura and K. Honjo, Jpn. J. Appl. Phys. **20**, Suppl. **3**, 17 (1980).

[9]L. A. Chernozatonskii and V. V. Novikov, Solid State Commun. **51**, 643 (1984).

[10]V. V. Novikov and L. A. Chernozatonskii, Fiz. Tverd. Tela (Leningrad) **28**, 419 (1986) [Sov. Phys. Solid State **28**, 233 (1986)].

[11]A preliminary report has been published; Al. A. Kolomenskii and A. A. Maznev, Pis'ma Zh. Eksp. Teor. Fiz. **53**, 403 (1991) [JETP Lett. **53**, 423 (1991)].

[12]*Akusticheskie Kristalli,* edited by M. P. Shaskol'skaya (Nauka, Moscow, 1982) (in Russian).

[13]T. L. Szabo and A. J. Slobodnik, Jr., IEEE Trans. Sonics Ultrason. **SU-20**, 240 (1973).

[14]Al. A. Kolomenskii and A. A. Maznev, Pis'ma Zh. Tekh. Fiz. **17**, 62 (1991) [Sov. Tech. Phys. Lett. **17** (1991)].

[15]H. Sontag and A. C. Tam, IEEE Trans. Ultrason. Ferroelectrics Freq. Cont. **UFFC-33**, 500 (1986).

[16]R. G. Pratt and T. C. Lim, Appl. Phys. Lett. **15**, 403 (1969).

[17]G. W. Farnell in *Physical Acoustics,* edited by W. P. Mason and R. N. Thurston (Academic, New York, 1970), Vol. VI.

[18]A. Neubrand, P. Hess, H. Coufal, and R. K. Grygier, in *Photoacoustic and Photothermal Phenomena III,* edited by D. Bićanić, Springer Series in Optical Sciences Vol. 69 (Springer-Verlag, Berlin, 1992), p. 317.

[19]I. A. Viktorov, *Rayleigh and Lamb Waves* (Plenum, New York, 1967).

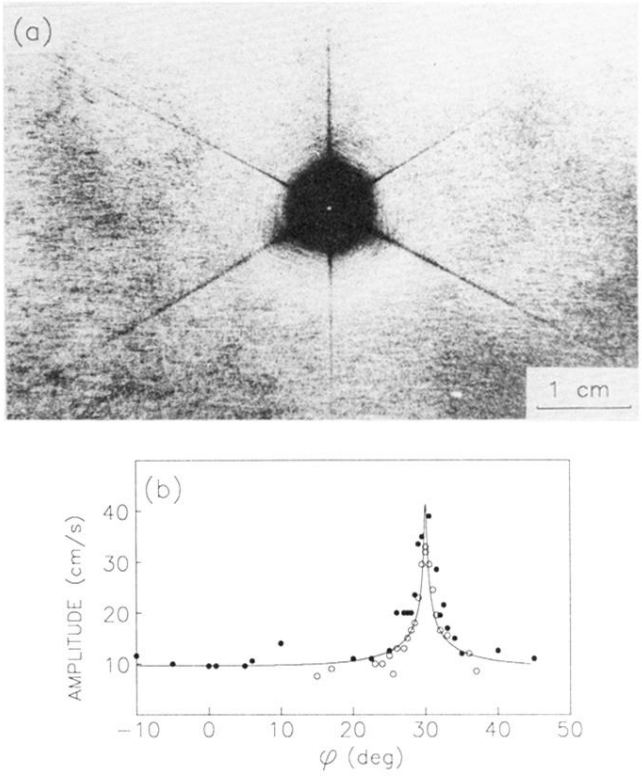

FIG. 1. Phonon focusing of SAW's in the (111) plane of silicon. (a) Focusing pattern: photograph of the dusted surface after laser-acoustic action. The ⟨110⟩ axis is horizontal. (b) Measured and calculated angular dependencies of the amplitude of the normal component of the surface velocity in a SAW pulse. The angle φ is measured from the ⟨110⟩ direction. The black and white circles refer to different series of measurements. For the calculated curve an arbitrary amplitude scale is used.

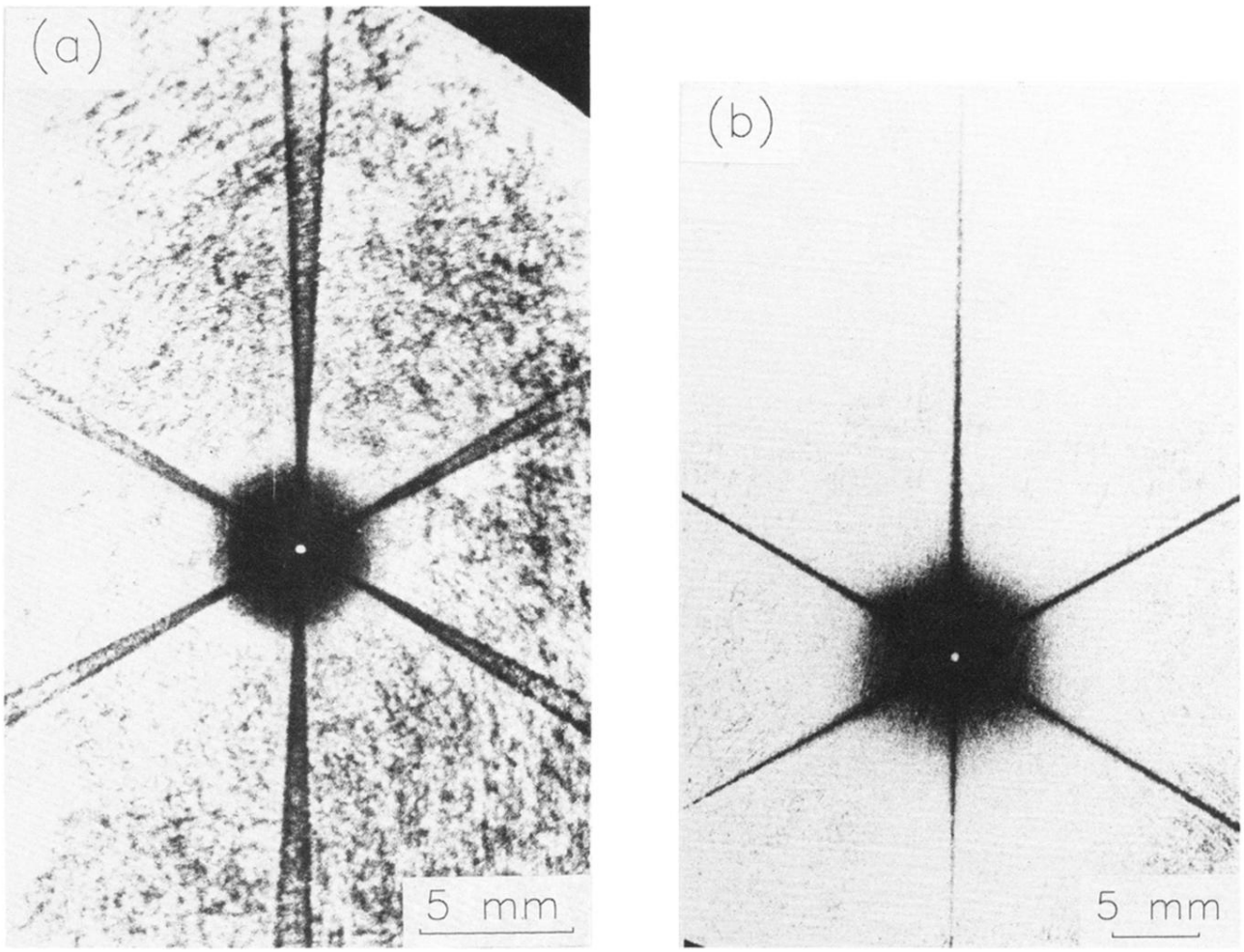

FIG. 3. Focusing patterns for the (111) surfaces of (a) GaAs and (b) germanium. The ⟨110⟩ axis is horizontal.

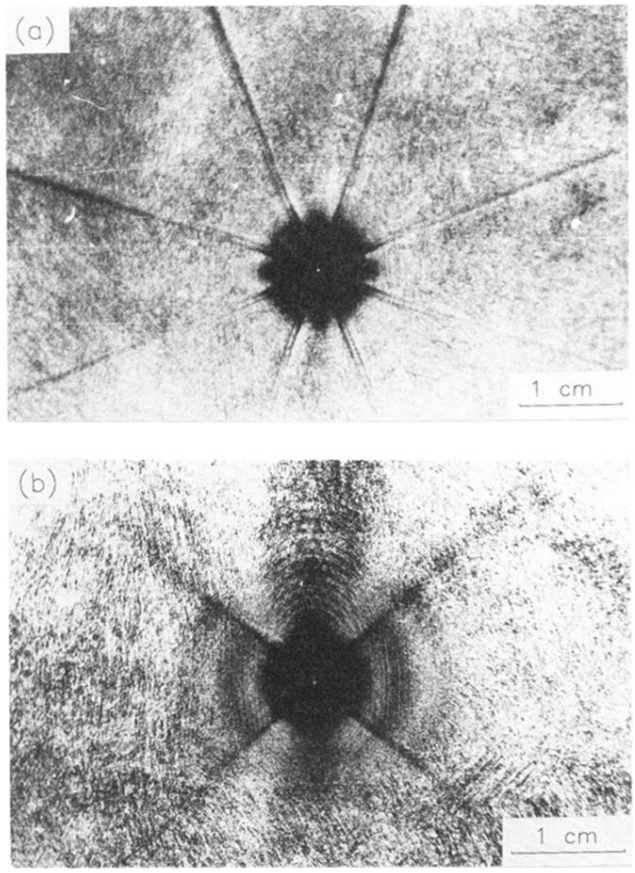

FIG. 4. Focusing patterns for the (a) (100) and (b) (110) surfaces of Si. In the both cases the ⟨110⟩ axis is horizontal.

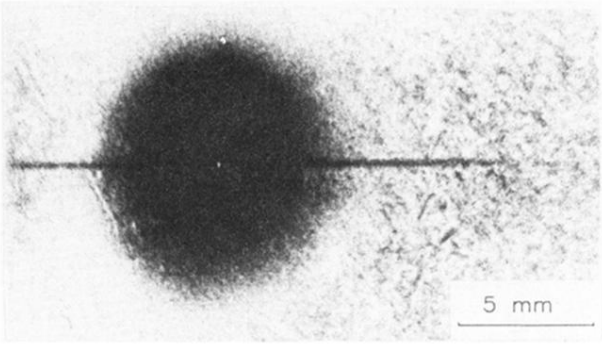

FIG. 6. Focusing pattern for the y cut of the $LiNbO_3$ crystal. The z axis is horizontal.